Journal of Environmental Chemical Engineering 2 (2014) 981–987

Contents lists available at ScienceDirect

Journal of Environmental Chemical Engineering

journal homepage: www.elsevier.com/locate/jece

Removal of Zn^{2+}, Fe^{2+}, Cu^{2+}, Pb^{2+}, Cd^{2+}, Ni^{2+} and Co^{2+} ions from aqueous solutions using modified phosphate dolomite

A.I. Ivanets[a,*], N.V. Kitikova[a], I.L. Shashkova[a], O.V. Oleksiienko[b], I. Levchuk[b], M. Sillanpää[b]

[a]Institute of General and Inorganic Chemistry of National Academy of Sciences of Belarus, st. Surganova 9/1, 220072 Minsk, Belarus
[b]Laboratory of Green Chemistry, Lappeenranta University of Technology, Sammonkatu 12, 50130 Mikkeli, Finland

ARTICLE INFO

Article history:
Received 10 December 2013
Accepted 24 March 2014

Keywords:
Phosphate dolomite
Metal ions
Adsorption
Isotherms

ABSTRACT

In the present work, modification of phosphate dolomite was conducted and applied for some bivalent metal ions removal. Physico-chemical properties of sorbent were characterized by means of X-ray diffraction (XRD), Fourier transform infrared spectroscopy (FTIR), differential-thermal analysis (DTA), thermogravimetric analysis (TGA), scanning electron microscopy (SEM) and low temperature adsorption–desorption of nitrogen. Sorption properties of modified dolomite for Zn^{2+}, Fe^{2+}, Cu^{2+}, Pb^{2+}, Cd^{2+}, Ni^{2+} and Co^{2+} removal were studied using model solutions. The highest removal efficiency was observed in pH range from 2 to 5. Among all tested metals, highest adsorption capacity of phosphated dolomite was detected towards Co^{2+} and Pb^{2+} (15 and 12 mmol g^{-1}, respectively) and the lowest towards Zn^{2+}, Fe^{2+} and Cu^{2+} (about 8 mmol g^{-1}). Adsorption isotherms were built for each tested metal ions and were fitted to Langmuir, Freundlich and Redlich–Peterson models.

Introduction

It is well known that bivalent metal ions pollution has become one of the most serious environmental problems today and elevated concentrations have been observed even in the most remote regions [1–3]. The number of methods such as ion exchange, membrane separation, electrolysis, chemical precipitation, and adsorption are used for removal metal ions from aqueous solutions [4–8]. Due to simplicity, effectiveness, and low cost adsorption is widely used technology for heavy metal ions removal [9]. As a rule it has been used as the main method for metal ions removal at low concentrations, or as a final polishing step. Some natural (dolomite, clay and related minerals, i.e., bentonites, montmorillonite, kaolinite [10–14]) or synthetic products (the nanosized metal oxides, metal phosphate, e.g., zirconium or hydroxyl apatite [15–17]) are known to be good adsorbents for metal ions and some of them have excellent ion-exchange properties. However, these materials have a low sorption capacity of 1–2 mmol g^{-1}, and they cannot always be used in acidic environments. Thus, there is a need for the search for novel highly effective sorbents for metal ions.

It has been demonstrated that calcium and magnesium phosphates of non-apatite structure synthesized from chemical reagents have a high sorption properties in processes of some metal ions removal from aqueous solutions [18]. As it was reported in [19], calcium and magnesium phosphates were obtained using natural dolomite – common and low-cost mineral consisting of magnesium and calcium carbonates. However, the obtained Ca–Mg phosphate sorbents were examined only towards Pb^{2+} ions and their sorption capacity was lower than that studied in [18].

The goal of present paper is to improve the method of synthesis of Ca–Mg phosphate sorbent using natural dolomite and to study its sorption properties towards Zn^{2+}, Fe^{2+}, Cu^{2+}, Pb^{2+}, Cd^{2+}, Ni^{2+} and Co^{2+} ions. The above mentioned metals were chosen based on content of real wastewaters from Zn–Cu mines.

Experimental

Preparation of sorbent

Dolomite from the Ruba deposit (Vitebsk region, Belarus) with the following chemical composition (wt.%): SiO_2 1.1, Fe_2O_3 0.4, Al_2O_3 0.5, CaO 30.3, MgO 20.0, SO_3 0.4, calcinations loss 47.0, K_2O 0.2, and Na_2O 0.1 was used as starting material for sorbent preparation. Ca–Mg phosphate was prepared by precipitation from aqueous solution as described in detail elsewhere [15] with several changes. For the synthesis of sorbent with a high content of calcium and magnesium phosphates and high sorption properties at the level of materials obtained in [18] it was previously suggested to activate the natural dolomite by its calcination at 800 °C. This will allow to remove organic impurities contained in the natural dolomite, and also to decompose the dolomites to the magnesium oxide and calcium carbonate [20], which will significantly improve its activity in interaction with nitric acid.

In contrast to previous work, the synthesis was realized by a slow controlled titration (5 mL s^{-1}), and after total addition of the ammonium phosphate solution the suspension was mated during 24 h.

* Corresponding author.
E-mail address: Ivanets@igic.bas-net.by (A.I. Ivanets).

2213-3437/$ - see front matter © 2014 Elsevier Ltd. All rights reserved.
http://dx.doi.org/10.1016/j.jece.2014.03.018

Table 1
Initial concentrations of metals in model solutions.

Metal	Cd^{2+}	Co^{2+}	Cu^{2+}	Fe^{2+}	Ni^{2+}	Pb^{2+}	Zn^{2+}
C (mg L^{-1})	133.7	93.7	94.4	89.5	96.8	2.7	123.1

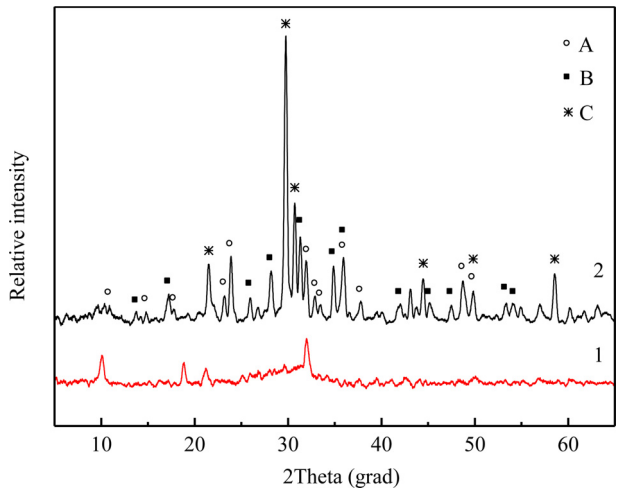

Fig. 1. X-ray diffraction patterns of Ca–Mg-phosphate after heating at 65 °C (1) and after calcination at 1000 °C (2). A – $Ca_4Mg_5(PO_4)_6$ (PDF No. 11-0231); B – $Ca_{2.81}Mg_{0.19}(PO_4)_2$ (PDF No. 70-682); C – $Mg_2P_2O_7$ (PDF No. 72-2042).

After the aging and washing with distilled water the precipitate of Ca–Mg phosphate was rinsed with ethanol. Replacement of intermicellar liquid (water–ethanol) allows to obtain the sorbent with a more developed mesoporous structure, because ethanol has a lower value of the surface tension than water.

Analytical methods

For elemental composition analysis, sorbent was dissolved in 6 M nitric acid. Total calcium and magnesium concentration was determined using complexometric EDTA-titration (±2%), magnesium concentration – by means of atomic-adsorption spectrometer (AAS) ontr AA 300 (Germany) (±3%). The concentration of PO_4^{3-} was defined spectrophotometrically as phosphovanadomolybdate complex at $\lambda = 440$ nm (±0.4%). Determination of nitrogen and carbon content was performed with the elemental analyzer Vario Micro. CHNS Mode (Elemetar Analysensysteme GmbH).

X-ray diffractometer (XRD) DRON-3 using Cu Kα radiation (2Θ 5–70°) was used for sorbent phase composition measurements. The morphology and the particle size of the sorbent were examined using a scanning electron microscope (SEM) JEOL-5610 LS (Japan). The Fourier transform infrared spectrum (FTIR) of the sample in KBr pellet was recorded on Midac Fourier transform infrared field spectrometer at room temperature in the range of 400–4000 m^{-1}.

DTA and TGA were performed by means of derivatograph system NETZSCH STA 409 PC/PG, when heated with a speed of 10 °/min from 20 to 1000 ° in air atmosphere.

The adsorption and texture properties of the sorbent were assessed by isotherms of low temperature (−196 °C) physical adsorption–desorption of nitrogen, measured by the volumetric method on an ASAP 2020 MP surface area and porosity analyzer (Micromeritics, US). The surface area of pores per unit mass of the solid or the specific surface area was determined by the methods of a single point (A_{sp}), BET (A_{BET}), and Langmuir (A_L). The single point method was used to calculate not only the specific surface area A_{sp}, but also the adsorption and desorption volumes ($V_{sp.ads}$ and $V_{sp.des}$) of pores and their average adsorption and desorption diameters D_{ads} and D_{des}. The cumulative adsorption and desorption volumes V_{BJHads} and V_{BJHdes} of pores with diameters in the range 1.7–300 nm, and the average adsorption and desorption pore diameters D_{BJHads} and D_{BJHdes} were calculated by the Barrett–Joyner–Halenda (BJH) method. The differential distribution of the mesopore volume over diameters, dV/d log D, was calculated by the Barrett–Joyner–Halenda method. The relative error in determining the pore volume was ±1% for the surface area and ±15% for the pore size.

Concentrations of metals in samples received during adsorption tests were determined by means of inductively coupled plasma optical emission spectrometer (ICP-OES) model iCAP 6300 (Thermo Electron Corporation, USA). Measurements of pH were carried out by means of pH meter 340i (±0.02).

Adsorption studies and modeling

Chemicals

Chemicals used for preparation of model solutions were $ZnSO_4{\cdot}6H_2O$, $FeSO_4{\cdot}7H_2O$, $CuSO_4{\cdot}5H_2O$, $Pb(NO_3)_2$, $CdSO_4$, $NiSO_4{\cdot}6H_2O$, $CoSO_4{\cdot}7H_2O$ and H_2SO_4, which were of analytical grade and utilized as purchased from Sigma–Aldrich without further purification. HNO_3 (Suprapur, 65%) was purchased from Merck Millipore International. Laboratory glassware was washed with strong HCl or HNO_3. For all experiments, Milli-Q water (resistance 18.2 MΩ cm^{-1}) was used.

Dose of sorbent

Purpose of this part of study was to determine the optimum dose of prepared sorbent for maximum removal of Zn^{2+}, Fe^{2+}, Cu^{2+}, Pb^{2+}, Cd^{2+}, Ni^{2+} and Co^{2+} from model solutions, initial concentrations of model solutions are presented in Table 1. Therefore, sorbent with concentrations in range from 0.5 g L^{-1} to 10 g L^{-1} were agitated with 20 mL of model solution (pH = 2.6) for 24 h using rotary shaker ST15 (CAT, M.Zipperer GmbH, Staufen, Germany). After that sorbent was filtered using 0.45 μm polypropylene syringe filter, concentration of metals in solutions was measured with ICP-OES.

Effect of pH on adsorption of metals

Influence of pH on the removal of metals using synthesized sorbent was studied in pH varying from 1 to 6. For pH adjustment H_2SO_4 (98%) and NaOH (5 M) solutions were used. Concentration of sorbent used in these tests was 10 g L^{-1}, volume of model solution, containing Zn^{2+}, Fe^{2+}, Cu^{2+}, Pb^{2+}, Cd^{2+}, Ni^{2+} and Co^{2+} was 10 mL and contact time was 24 h.

Study of metal ions sorption in time

In this study, during which 0.2 g of sorbent was mixed with 20 mL of model solution with pH 2.6 was conducted at ambient temperature. Concentration of metals was measured in samples taken at desired time.

Adsorption isotherms for one-component systems

Experiments were conducted at room temperature for 24 h and volume of 10 mL of model solution was mixed with 0.1 g of sorbent material. Single component model solutions of Zn^{2+}, Fe^{2+}, Cu^{2+}, Pb^{2+}, Cd^{2+}, Ni^{2+} and Co^{2+} with initial concentrations ranging from 0.1 to 2.0 g L^{-1} were tested. Data obtained from these experiments were used for building adsorption equilibrium isotherms in accordance with Langmuir, Freundlich and Redlich–Peterson models,

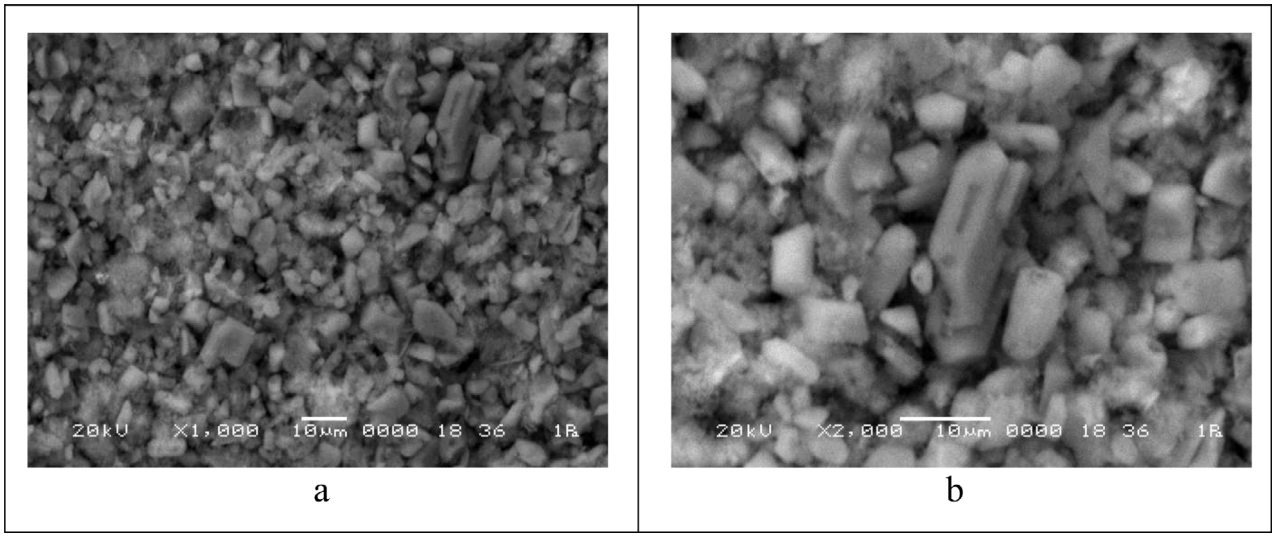

Fig. 2. SEM micrographs of Ca–Mg phosphate after heating at 65 °C, magnified 1000 × (a) and 2000 × (b).

Table 2
Adsorption properties (specific surface area, pore volume and pore diameter) of the sorbent.

Specific surface area ($m^2\ g^{-1}$)			Pore volume ($cm^3\ g^{-1}$)				Pore diameter (nm)			
A_{sp}	A_{BET}	A_L	$V_{sp\ ads}$	$V_{sp\ des}$	$V_{BJH\ ads}$	$V_{BJH\ des}$	$D_{sp\ ads}$	$D_{sp\ des}$	$D_{BJH\ ads}$	$D_{BJH\ des}$
49	54	78	0.182	0.238	0.270	0.272	15	19	23	16

Table 3
Parameters of isotherms.

Metal	Langmuir				Freundlich			
	$q_{exp.}$ (mmol g^{-1})	$q_{calc.}$ (mmol g^{-1})	K_L	R^2	$q_{calc.}$ (mmol g^{-1})	K_F	n	R^2
Cd^{2+}	10.88	6.78	4.23	0.778	9.62	2.30	3.25	0.945
Co^{2+}	15.12	14.19	0.06	0.950	16.68	2.71	3.68	0.961
Cu^{2+}	8.68	7.81	10.07	0.983	9.08	3.30	4.49	0.962
Fe^{2+}	8.37	8.38	2038.14	0.880	8.97	5.49	9.57	0.742
Ni^{2+}	9.35	8.76	0.27	0.944	9.86	2.38	3.47	0.983
Pb^{2+}	12.42	11.49	832.98	0.911	13.13	6.34	8.29	0.704
Zn^{2+}	7.84	7.58	45.48	0.987	8.92	4.08	5.73	0.890

Metal	**Redlich–Peterson**				
	$q_{exp.}$ (mmol g^{-1})	$q_{calc.}$ (mmol g^{-1})	K_{RP}	n_{RP}	R^2
Cd^{2+}	10.88	9.60	9928.0	0.70	0.944
Co^{2+}	15.12	15.70	1.33	0.81	0.992
Cu^{2+}	8.68	8.49	26.73	0.90	0.998
Fe^{2+}	8.37	7.76	768.24	1.07	0.896
Ni^{2+}	9.35	9.59	6.87	0.77	0.992
Pb^{2+}	12.42	11.81	600.20	1.02	0.915
Zn^{2+}	7.84	7.65	49.22	0.99	0.987

which are basically used for the description of adsorption of single component. All isotherms used in this study are presented below [21]:

Langmuir:

$$q_e = \frac{q_m K_L C_e}{1 + K_L C_e} \quad (1)$$

where q_e and C_e are the adsorption capacity (mmol g^{-1}) and the equilibrium concentration of the adsorbate (mmol L^{-1}) respectively, while q_m and K_L represent the maximum adsorption capacity of adsorbents (mmol g^{-1}) and the energy of the adsorption (L $mmol^{-1}$) respectively.

Freundlich:

$$q_e = K_F C_e^{1/n_F} \quad (2)$$

where K_F ((mmol g^{-1})/(L $mmol^{-1})^n{}_F$) and n_F are the Freundlich adsorption constants.

Redlich–Peterson:

$$q_e = \frac{q_m K_{RP} C_e}{1 + (K_{RP} C_e)^{n_{RP}}} \quad (3)$$

where K_{RP} and n_{RP} are the Redlich–Peterson constants.

Fitting of experimental data with mentioned models were carried out using the solver add-in with Microsoft's spreadsheet, Microsoft Excel. In order to check accuracy of the experimental data fitting by isotherms the coefficient of determination (R^2) presented below was

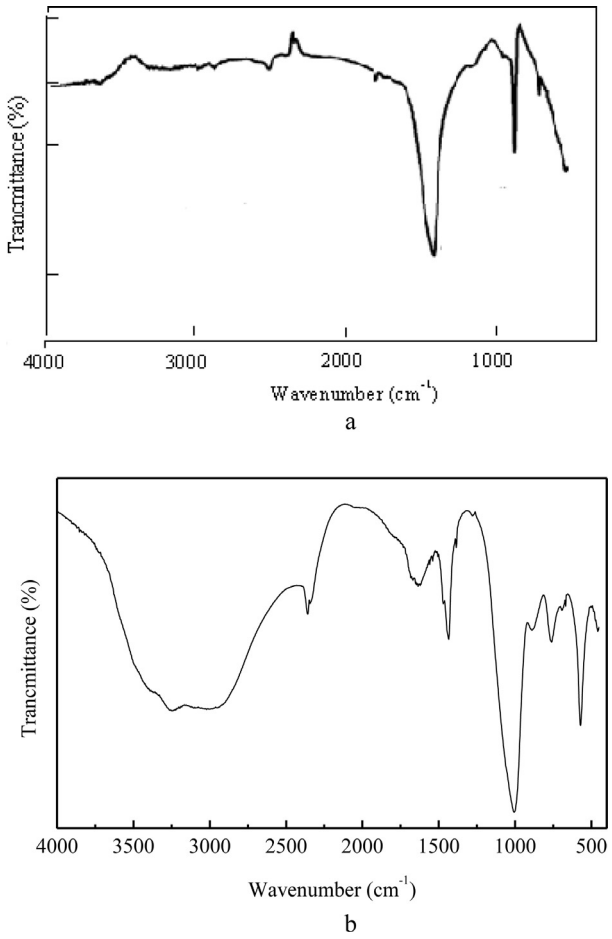

Fig. 3. FTIR spectrum of initial dolomite (a) and Ca–Mg-phosphate after heating at 65 °C (b).

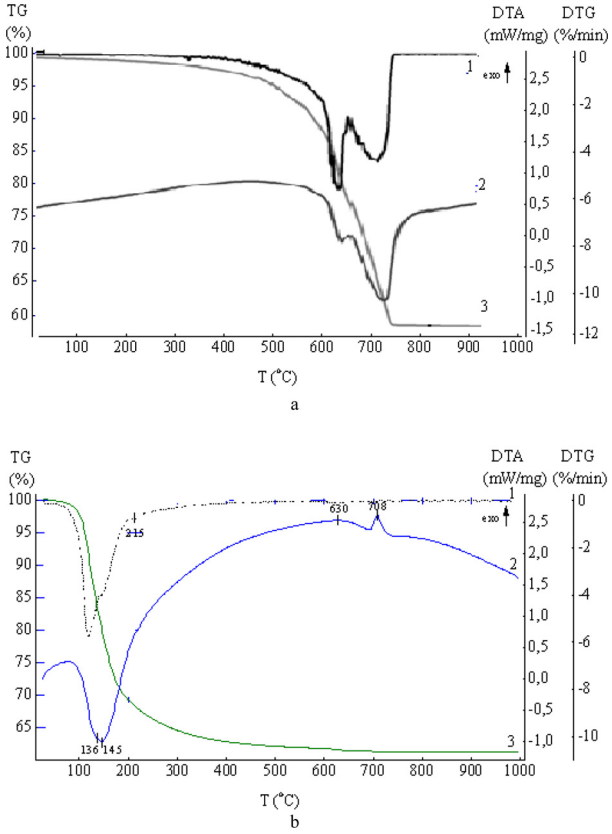

Fig. 4. DTG (1), DTA (2) and TG (3) curves for initial dolomite (a) and Ca–Mg-phosphate sample (b).

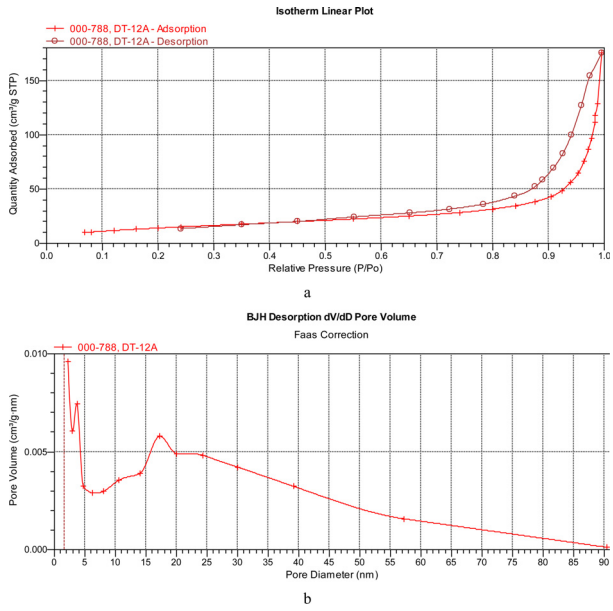

Fig. 5. Isotherms of low-temperature adsorption–desorption of nitrogen in the linear form (a) and pore diameter distribution curves d*V*/d*D*–*D* plotted using BJH method (b) for the sorbent synthesized.

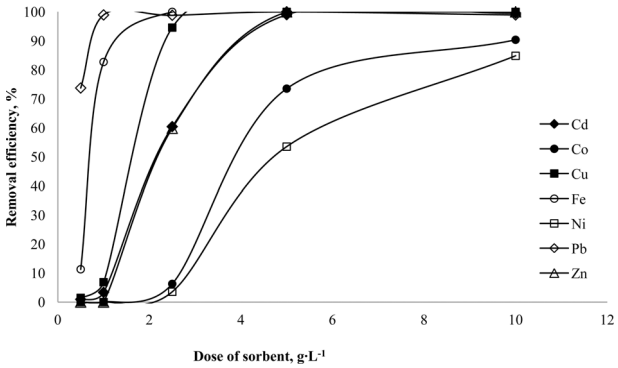

Fig. 6. Dependence of metal removal efficiency on concentration of sorbent.

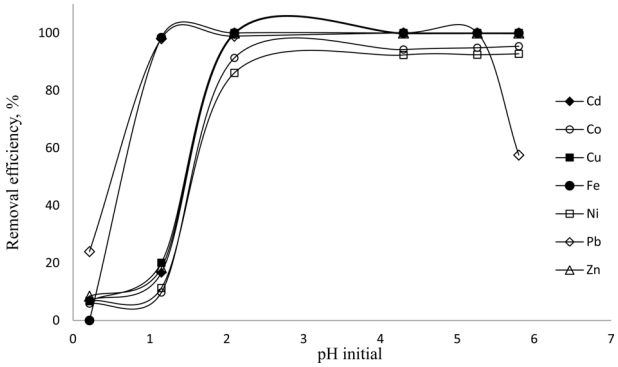

Fig. 7. Elimination of Zn^{2+}, Fe^{2+}, Cu^{2+}, Pb^{2+}, Cd^{2+}, Ni^{2+} and Co^{2+} at various initial pH. Contact time 24 h, dose of sorbent 10 g L^{-1}.

applied.

$$R^2 = \frac{\Sigma(q_{e,exp} - \overline{q}_{e,exp})^2 - \Sigma(q_{e,exp} - \overline{q}_{e,calc})^2}{\Sigma(q_{e,exp} - \overline{q}_{e,exp})^2} \quad (4)$$

where $q_{e,calc}$ is equilibrium capacity, calculated from isotherm equation, $q_{e,exp}$ is equilibrium capacity obtained experimentally and $\overline{q}_{e,exp}$ is mean value of $q_{e,exp}$.

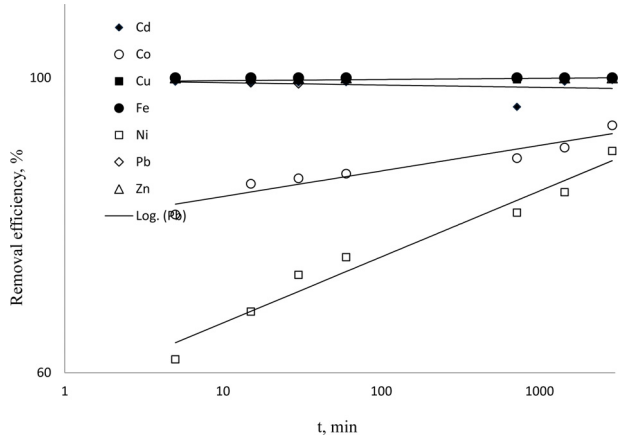

Fig. 8. Dependence of metal removal efficiency on contact time, dose of sorbent 10 g L^{-1}, pH of solution was 2.6.

Results and discussion

Characterization of material

Summing up data of elemental analysis, the composition of prepared sorbent can be described with formula $_3Mg_2(NH_4)_{1.3}(PO_4)_4(CO_3)_{0.3}{\cdot}6H_2O$. The presence of ammonia groups could explain the fact of calcium and magnesium phosphates precipitation performed by ammonia solution. As a result, the obtained sorbent includes the impurities of phase $MgNH_4PO_4{\cdot}6H_2O$ (struvite). The low content of CO_3^{2-} ions in sorbent confirms the almost complete transformation of dolomite to calcium and magnesium phosphates.

The chemical composition is confirmed by the data of the physicochemical analytical methods. From XRD data it can be seen that sorbent is at amorphous state (Fig. 1, curve 1).

As result of heat treatment of sorbent with formula $_3Mg_2(NH_4)_{1.3}(PO_4)_4(CO_3)_{0.3}{\cdot}6H_2O$ at 1000 °, phases , and were crystallized, where and are binary Ca–Mg phosphate with Ca:Mg = 4:5 and Ca:Mg = 2,81:0.19, respectively, is magnesium pyrophosphate – the main product of polymerization of HPO_4^{2-} anion forming after the NH_3 removal from struvite (Fig. 1, curve 2).

$$MgNH_4PO_4 \cdot 6H_2O \rightarrow MgHPO_4 \cdot nH_2O + NH_3 \uparrow \rightarrow Mg_2P_2O_7 + H_2O \quad (5)$$

The low crystallinity and the heterogeneity of composition were confirmed using SEM (Fig. 2). The electron micrographs show that sorbent consisted of both, little oval particles with average dimensions around 2–4 μm and their aggregates and small crystals with a length of 10–16 μm and diameter of 6 μm. Such crystal form is typical for struvite. [22,23]

Fig. 3 shows FTIR spectrums of initial dolomite and after phosphate. The spectrum of Ca–Mg phosphate sample (3b) contains not only the phosphate bands at 570 and 1000 cm^{-1}, but also the bands of NH_4^+ group at 1380, 1435 and 1470 cm^{-1}. The rest bands are attributed to hydrogen bonds of water–phosphate or water–NH_4^+ group [24]. The form of spectrum suggests the amorphous state of the sorbent. The phosphate groups have the unresolved bands that are typical for a poorly crystalline phosphate phase. The O_3^{2-} group has several bands in the same range as NH_4^+ group but carbonate content is very low, therefore, it cannot be observed at FTIR spectrum.

The DTA, DTG and TG curves for the initial dolomite and obtained sample are presented in Fig. 4. The DTA curve (Fig. 4b) shows two endothermic peaks at 136 and 145 °C and exothermic peaks around 630 and at 708 °C. The DTG curve has additional small peak at 215 °C. The peaks at 145, 215 and 630 °C are attributed to the removal of water, then the removal of the ammonia and the formation of $Mg_2P_2O_7$, respectively [24–26]. The peaks at 136 and 708 °C correspond to the removal of crystal hydrate water and the crystallization of Ca- and Mg phosphates [27]. The phases observed by XRD after heating of the sample correspond to thermal analysis data (Fig. 1, curve 2). Thus, it was established that after thermal treatment sorbent consists of mixture of $Mg_2P_2O_7$ and two phosphatic phases, such as $Ca_4Mg_5(PO_4)_6$ and $Ca_{2.81}Mg_{0.19}(PO_4)_2$.

The sorption isotherm in Fig. 5a is mostly type IV and demonstrate that the sample belongs to mesoporous structures. The hysteresis loop in the isotherms is type N3 according to the IUPAC classification. Analysis of the differential curves of the pore diameter distributions by the BJH method (Fig. 5b) makes it possible to identify a mesoporous structure with a predominant pore diameter of 15–20 nm and 2–4 nm.

According to the data from Table 2 the mesopore volumes by single point (ads/des) and BJH (ads/des) are 0.182/0.238 and 0.270/0.272 $cm^3\ g^{-1}$ and the specific surface areas by single point, BET and Langmuir are 49, 54 and 78 $m^2\ g^{-1}$, respectively. The average pore diameter calculated by single point and BJH methods are in the range 15–23 nm.

Adsorption studies

Dose of sorbent

According to Fig. 6, removal efficiency of Fe^{2+}, Pb^{2+} and Cu^{2+} is higher than 90% at sorbent concentration around 2 g L^{-1}. The efficient removal of Zn^{2+} and Cd^{2+} is reached at sorbent dose 5 g L^{-1}. The removal efficiency of Co^{2+} and Ni^{2+} is the lowest from all tested metals – less than 85%. Taking into account that at concentration of sorbent equal to 10 g L^{-1} removal efficiency of all tested metals was the highest, this sorbent dose was chosen as optimum for further studies.

Effect of pH

Aim of this part of study was to determine optimum pH conditions for efficient elimination of all metals presented in model solution. In previous paper [18] it was shown that the removal of bivalent metal ions follows complex mechanism which included physical adsorption, ion exchange and chemisorption. The polyvalent ions interact with Ca–Mg phosphate and obtain compounds with low solubility. It is also clear that different pH of initial solutions determines a different state of metal ions in solution.

Results, which are shown in Fig. 7, suggest that highest removal efficiency for all considered metals was observed within pH range from 2 to 5, which is relatively wide and can be beneficial for the treatment of different types of wastewaters. Fe^{2+} and Pb^{2+} adsorption had the widest pH range – from 1 to 6 and 1–5.2, respectively. The optimal pH value provides the condition for the maximum extraction of polyvalent metal ions from solution. The low efficiency of metal ions removal at pH < 2 was connected with the increased solubility as phosphate-sorbent, and the product of its interaction.

Study of metal ions sorption in time

In order to find out required time for achieving equilibrium, this study was carried out. Model solution was used for this purpose. Samples were taken after 5, 15, 30, 60, 720, 1440 and 2880 min. In Fig. 8 removal efficiency of metals depending on sampling time was shown. As it can be noticed from this plot, already after 5 min of experiment such metals as Cd^{2+}, Cu^{2+}, Fe^{2+}, Pb^{2+} and Zn^{2+} were removed completely. Whereas, sorption of Co^{2+} and Ni^{2+} was not so fast, achieving highest elimination of abovementioned metals after 2880 min. This fact probably related to ionic radii: the kinetics of metal cations slowed with decreases of the ionic radii.

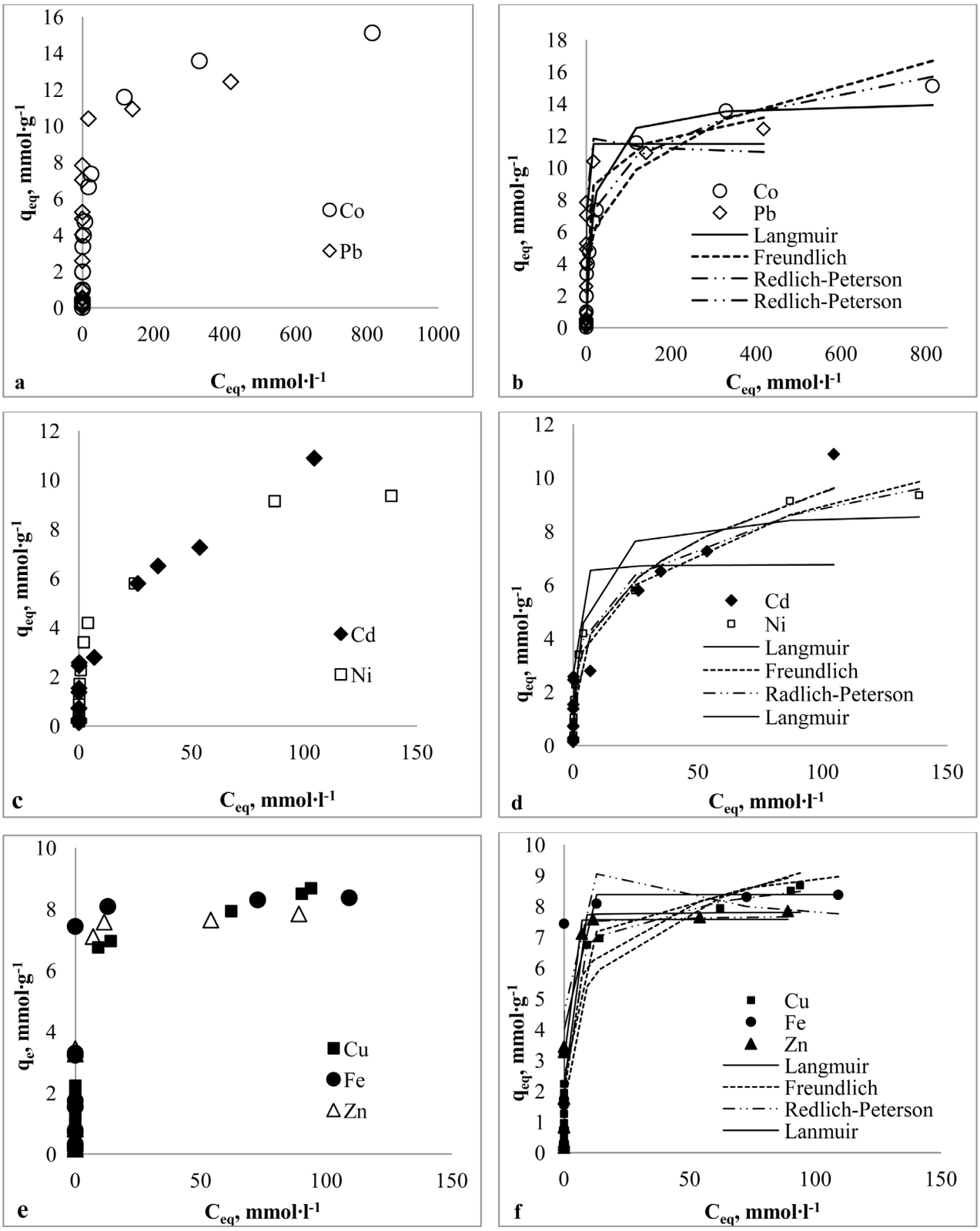

Fig. 9. Adsorption isotherms of cations from aqueous solution. Contact time 24 h, dose of sorbent 10 g L^{-1}, pH of solution 2.6.

Adsorption isotherms

Adsorption isotherms were obtained for each of the following metals: Zn^{2+}, Fe^{2+}, Cu^{2+}, Pb^{2+}, Cd^{2+}, Ni^{2+} and Co^{2+} at different initial concentrations (Fig. 9, curves a, c, and e). All isotherms belong to H type according to Giles classification of adsorption on solids from liquids. This is a case in which the solute has such high affinity that in dilute solutions it is adsorbed completely or till trace amount, which are difficult to detect. It was found that adsorption affinity towards metal cations increases with the rise of the ionic radius. The effect of ionic radii was observed in [28]. The selectivity range of metals for synthesized material can be presented as Ni < Co < Zn ~ Fe ~ Cu ~ Cd ~ Pb at low concentration (100 mg L^{-1}) from both model aqueous solutions (Figs. 7 and 8). At higher metal concentrations, the selectivity range changes and can be shown in following form Zn < Fe < Cu < Ni < Cd < Pb < Co. The increasing of maximum adsorption of Ni^{2+} and Co^{2+} could be arised as a summing result of the following factors: 1 – the complex composition of adsorbent (consisting of three cations and two anions), 2 – different forms of finding the ions of these metals in solution; 3 – features of the mechanism of interaction of various metal ions with a sorbent; 4 – different solubility of compound formed as a results of interactions. For example, in works [29–31] observed hiding of adsorption range from directly-proportional of radii either.

Equilibrium data were fit to Langmuir, Freundlich and Redlich–Peterson models (Fig. 9, curves b, d, and f). As it can be seen from Table 3, experimental data can be described more precisely with Redlich–Peterson model for Zn^{2+}, Cu^{2+}, Ni^{2+} and Co^{2+}. The complexity of choosing models for cadmium Cd^{2+}, Fe^{2+} and Pb^{2+} sorption by synthesized sorbent arises due to the complex mechanism of sorption.

Conclusion

The sorption material with high content of calcium and magnesium was synthesized from natural dolomite using the improved method. According to results of physico-chemical analysis established that composition of prepared sorbent can be described with formula $_3Mg_2(NH_4)_{1.3}(PO_4)_4(CO_3)_{0.3}\cdot 6H_2O$, sorbent has a low crystallinity and developed mesopore structure.

The adsorption studies showed the high sorption properties towards Zn^{2+}, Fe^{2+}, Cu^{2+}, Pb^{2+}, Cd^{2+}, Ni^{2+} and Co^{2+} ions. The highest removal efficiency of chosen metal ions was observed in pH range from 2 to 5 with adsorbent concentration in model solution equal to 10 mg L^{-1}. It was established that obtained material has maximum adsorption capacity (up to 12–15 mmol g^{-1}) towards Co^{2+} and Pb^{2+}, while the adsorption of Co^{2+} and Ni^{2+} were the slowest among the rest cations. Collected data allows to conclude that prepared material can be used as an effective adsorbent for divalent metal cations from acidic water aqueous solutions.

References

[1] F. Fu, Q. Wang, Removal of heavy metal ions from wastewaters: a review, Journal of Environmental Management 92 (2011) 407–18. http://dx.doi.org/10.1016/j.jenvman.2010.11.011, 21138785.

[2] X. Huang, M. Sillanpää, B. Duo, E.T. Gjessing, Water quality in the Tibetan plateau: metal contents of four selected rivers, Environmental Pollution 156 (2008) 270–7. http://dx.doi.org/10.1016/j.envpol.2008.02.014, 18375027.

[3] X. Huang, M. Sillanpää, E.T. Gjessing, R.D. Vogt, Water quality in the Tibetan plateau: major ions and trace elements in the headwaters of four major Asian rivers, Science of the Total Environment 407 (2009) 6242–54. http://dx.doi.org/10.1016/j.scitotenv.2009.09.001, 19783282.

[4] L. Zhang, Y.-H. Zhao, R. Bai, Development of multifunction membrane for chromatic warning and enhanced adsorptive removal of heavy metal ions: application to cadmium, Journal of Membrane Science 379 (2011) 69–79. http://dx.doi.org/10.1016/j.memsci.2011.05.044.

[5] S.O. Kim, S.H. Moon, K.W. Kim, S.T. Yun, Pilot scale study on the ex situ electrokinetic removal of heavy metals from municipal wastewater sludges, Water Research 36 (2002) 4765–74. http://dx.doi.org/10.1016/S0043-1354(02)00141-0, 12448519.

[6] M.J.S. Yabe, E. Oliveria, Heavy metal removal in industrial effluents by sequential adsorbent treatment, Advanced in Environmental Research 7 (2003) 263–72. http://dx.doi.org/10.1016/S1093-0191(01)00128-9.

[7] S.-F. Lo, S.-Y. Wang, M.-J. Tsai, L.-D. Lin, Adsorption capacity and removal efficiency of heavy metal ions by Moso and Ma bamboo activated carbons, Chemical Engineering Research and Design 90 (2012) 1397–406. http://dx.doi.org/10.1016/j.cherd.2011.11.020.

[8] C. Blöcher, J. Dorda, V. Mavrov, H. Chmiel, N.K. Lazaridis, K.A. Matis, Hybrid flotation—membrane filtration process for the removal of heavy metal ions from wastewater, Water Research 37 (2003) 4018–26. http://dx.doi.org/10.1016/S0043-1354(03)00314-2, 12909122.

[9] S. Babel, T.A. Kurniawan, Low-cost adsorbents for heavy metals uptake from contaminated water: a review, Journal of Hazardous Materials 97 (2003) 219–43. http://dx.doi.org/10.1016/S0304-3894(02)00263-7, 12573840.

[10] G.M. Walker, G. Connor, S.J. Allen, Copper(II) removal onto dolomitic sorbents, Chemical Engineering Research and Design 82 (2004) 961–6. http://dx.doi.org/10.1205/0263876041580712.

[11] E. Pehlivan, A.M. Özkan, S. Dinç, Ş. Parlayici, Adsorption of Cu^{2+} and Pb^{2+} ion on dolomite powder, Journal of Hazardous Materials 167 (2009) 1044–9. http://dx.doi.org/10.1016/j.jhazmat.2009.01.096, 19237240.

[12] K.G. Bhattacharyya, S.S. Gupta, Adsorption of a few heavy metals on natural and modified kaolinite and montmorillonite: a review, Advances in Colloid and Interface Science 140 (2008) 114–31. http://dx.doi.org/10.1016/j.cis.2007.12.008, 18319190.

[13] M.G.A. Vieira, A.F.A. Neto, M.L. Gimenes, Removal of nickel on Bofe bentonite calcined clay in porous bed, Journal of Hazardous Materials 176 (2010) 109–18, .

[14] S.M.I. Sajidu, I. Persson, W.R.L. Masamba, et al. Mechanisms of heavy metal sorption on alkaline clays from Tundulu in Malawi as determined by EXAFS, Journal of Hazardous Materials 158 (2008) 401–9. http://dx.doi.org/10.1016/j.jhazmat.2008.01.087, 18329799.

[15] M. Hua, Sh. Zhang, B. Pan, Heavy metal removal from water/wastewater by nanosized metal oxides: a review, Journal of Hazardous Materials 211–212 (2012) 317–31, .

[16] B. Pan, Q. Zhang, W. Du, et al. Selective heavy metals removal from waters by amorphous zirconium phosphate: behavior and mechanism, Water Research 41 (2007) 3103–11. http://dx.doi.org/10.1016/j.watres.2007.03.004, 17433402.

[17] A. Aklil, M. Mouflih, S. Sebti, Removal of heavy metal ions from water by using calcined phosphate as a new adsorbent, Journal of Hazardous Materials 112 (2004) 183–90. http://dx.doi.org/10.1016/j.jhazmat.2004.05.018, 15302439.

[18] I.L. Shashkova, A.I. Rat'ko, N.V. Kitikova, Removal of heavy metal ions from aqueous solutions by alkaline-earth metal phosphate, Colloids and Surfaces, Part A 160 (1999) 207–15. http://dx.doi.org/10.1016/S0927-7757(99)00193-4.

[19] N.V. Kitikova, I.L. Shashkova, A.I. Rat'ko, Synthesis of calcium and magnesium phosphates from natural carbonates and study of their activity in reactions with lead(II) ions, Russian Journal of Applied Chemistry 76 (2003) 368–73. http://dx.doi.org/10.1023/A:1025632213519.

[20] A.I. Rat'ko, A.I. Ivanets, A.I. Kulak, et al. Thermal decomposition of natural dolomite, Journal of Inorganic Materials 47 (2011) 1372–7. http://dx.doi.org/10.1134/S0020168511120156.

[21] K.Y. Foo, B.H. Hameed, A review: insights into the modeling of adsorption isotherm systems, Chemical Engineering Journal 156 (2010) 2–10. http://dx.doi.org/10.1016/j.cej.2009.09.013.

[22] L.N. Schegrov, Phosphaty Dvyhvalentnyh Metallov, Kiev, Nauk. Dumka, 1987, p. 216.

[23] E. Banks, R. Chianelli, R. Korenstein, Crystal chemistry of struvite analogs of the type $MgMPO_4\cdot 6H_2O$ ($M^+ = K^+$, Rb^+, Cs^+, Tl^+, NH_4^+), Inorganic Chemistry 14 (1975) 1634–9. http://dx.doi.org/10.1021/ic50149a041.

[24] E. Vorndran, A. Ewald, F.A. Müller, et al. Formation and properties of magnesium–ammonium–phosphate hexahydrate biocements in the Ca–Mg–PO_4 system, Journal of Materials Science: Materials in Medicine 22 (2011) 429–36. http://dx.doi.org/10.1007/s10856-010-4220-4.

[25] F. Abbona, A. Baronnet, A XRD and TEM study on the transformation of amorphous calcium phosphate in the presence of magnesium, Journal of Crystal Growth 165 (1996) 98–105. http://dx.doi.org/10.1016/0022-0248(96)00156-X.

[26] R.N. Panda, M.F. Hsieh, R.J. Chung, T.S. Chin, FTIR, XRD, SEM and solid state NMR investigations of carbonate-containing hydroxyapatite nano-particles synthesized by hydroxide-gel technique, Journal of Physics and Chemistry of Solids 64 (2003) 193–9. http://dx.doi.org/10.1016/S0022-3697(02)00257-3.

[27] V.A. Sinyaev, E.S. Shustikova, L.V. Levchenko, et al. Nature and thermal behavior of precipitated calcium–magnesium phosphates, Russian Journal of Applied Chemistry 76 (2003) 1375–9. http://dx.doi.org/10.1023/B:RJAC.0000012650.94921.ee.

[28] E.R. Nightingale, Phenomenological theory of ion solvation. Effective radii of hydrated ions, Journal of Chemical Physics 63 (1959) 1381–8. http://dx.doi.org/10.1021/j150579a011.

[29] J.H. Choi, S.D. Kim, Y.J. Kwon, W.J. Kim, Adsorption behaviors of ETS-10 and its variant, ETAS-10 on the removal of heavy metals, Cu^{2+}, Co^{2+},Mn^{2+} and Zn^{2+} from a waste water, Microporous and Mesoporous Materials 96 (2006) 157–67. http://dx.doi.org/10.1016/j.micromeso.2006.03.050.

[30] M.G. Klimantavièiûtë, D. Virbalytë, V. Pakðtas, R. Juðkënas, A. Pigaga, Interaction of heavy metal ions with cement kiln dust, Ekologija 1 (2005) 31–6.

[31] P. Tzvetkova, R. Nickolov, Modified and unmodified silica gel used for heavy metal ions removal from aqueous solutions, Journal of the University of Chemical Technology and Metallurgy 47 (2012) 498–504.